Cell Motility and the Cytoskeleton 57:207–217 (2004)

Measurement of Barbed Ends, Actin Polymerization, and Motility in Live Carcinoma Cells After Growth Factor Stimulation

Mike Lorenz, Vera DesMarais, Frank Macaluso, Robert H. Singer, and John Condeelis*

Albert Einstein College of Medicine, Department of Anatomy and Structural Biology, Bronx, New York

Motility is associated with the ability to extend F-actin-rich protrusions and depends on free barbed ends as new actin polymerization sites. To understand the function and regulation of different proteins involved in the process of generating barbed ends, e.g., cofilin and Arp2/3, fixed cell approaches have been used to determine the relative barbed end concentration in cells. The major disadvantages of these approaches are permeabilization and fixation of cells. In this work, we describe a new live-cell time-lapse microscopy assay to determine the increase of barbed ends after cell stimulation that does not use permeabilization and provides a better time resolution. We established a metastatic carcinoma cell line (MTLn3) stably expressing GFP-β-actin at physiological levels. Stimulation of MTLn3 cells with epidermal growth factor (EGF) causes rapid and transient lamellipod protrusion along with an increase in actin polymerization at the leading edge, which can be followed in live cell experiments. By measuring the increase of F-actin at the leading edge vs. time, we were able to determine the relative increase of barbed ends after stimulation with a high temporal resolution. The F-actin as well as the barbed end concentration agrees well with published data for this cell line. Using this newly developed assay, a decrease in lamellipod extension and a large reduction of barbed ends was documented after microinjecting an anti-cofilin function blocking antibody. This assay has a high potential for applications where rapid changes in the dynamic filament population are to be measured. Cell Motil. Cytoskeleton 57:207–217, 2004.

Key words: cytoskeleton; cofilin, fluorescence; GFP; microscopy

INTRODUCTION

Cell motility plays an important role in many biological processes, e.g., embryogenesis, neurite growth, wound healing, inflammation, or cancer metastasis. Motility is associated with the ability to extend F-actin-rich protrusions and requires cycles of actin polymerization and depolymerization (actin polymerization transients). Previous studies have demonstrated that free barbed ends define the location of actin polymerization in vivo [reviewed in Condeelis 2001].

There are three different mechanisms to generate free barbed ends: (1) uncapping of pre-existing barbed ends by capping protein or gelsolin [Hartwig et al., 1995] (2) severing of actin filaments by cofilin [Chan et al., 2000], or (3) de novo nucleation of new filaments involving the Arp2/3 complex [Pollard et al., 2000] or formins [Pruyne et al., 2002]. To understand the function and interaction of all the proteins involved in these dif-

The supplemental material referred to in this section can be found at: http://www.interscience.wiley.com/jpages/0886-1544/suppmat/index.html

Contract grant sponsor: NIH.

*Correspondence to: Dr. John Condeelis, Albert Einstein College of Medicine, Department of Anatomy and Structural Biology, 1300 Morris Park Avenue, Bronx, NY, 10461. E-mail: condeeli@aecom.yu.edu

Received 26 June 2003; Accepted 2 December 2003

ferent processes of free barbed end formation, the determination of the number of barbed ends at different times after stimulation in different regions of the cell is essential. Several approaches have been used to determine the relative barbed end concentrations in cells. In time-resolved fixation experiments, permeabilized cells are allowed to incorporate labeled actin monomers into filaments in situ to detect free barbed ends at different times of stimulation [Chan et al., 1998; Symons and Mitchison, 1991]. The resolution of this method has been extended to the electron microscope level of resolution [Bailly et al., 1999]. In photoactivation and photobleaching experiments, the redistribution of fluorescently labeled actin is followed to measure filament appearance and turnover [Theriot and Mitchison, 1992]. Fluorescence speckle microscopy has been used to provide fiduciary marks to follow the appearance and disappearance of actin filaments in vivo [Watanabe and Mitchison, 2002; Waterman-Storer and Salmon, 1997]. All of these methods have been informative and indicate that the most dynamic actin filaments are at the leading edge of cell surface protrusions.

However, all of these approaches suffer from disadvantages that make the analysis of barbed ends in vivo problematic. Time-resolved fixation experiments are capable of the highest resolution but suffer from potential artifacts due to the permeabilization step that can extract proteins involved in the nucleation process and the dynamic filament population at the leading edge. In addition, the requirement for permeabilization may delocalize the filaments that survive. Photoactivation and photobleaching experiments suffer from poor spatial resolution and uncertainties regarding interpretation of fluorescence due to reincorporation of disassembled actin subunits in vivo. Fluorescence speckle microscopy does not measure barbed ends directly and gives only relative information.

In the current study, we have adopted an approach to circumvent several of the disadvantages of these other techniques. We have used live cell fluorescence time-lapse microscopy to follow the rate of GFP-actin accumulation. This method does not require permeabilization, can be done in live cells, and detects the regions within cells containing free barbed ends with a high temporal resolution.

MATERIALS AND METHODS

Cell Lines

MTLn3 cells were cultured as described previously [Bailly et al., 1998a; Segall et al., 1996]. To generate cells expressing β-actin-EGFP, MTLn3 cells were transfected with plasmid pβ-actin EGFP (this plasmid contains the β-actin promoter followed by EGFP and β-actin) [Ballestrem et al., 1998]. Briefly, 1 μg of plasmid DNA and 10 μl of lipofectamine were incubated in 100 μl α-MEM (Gibco BRL, Gaithersburg, MD) for 45 min. The solution was diluted with 800 μl of α-MEM and added to 50–80% confluent MTLn3 cells in 35-mm culture dishes. After 1 h of incubation, the DNA solution was removed and replaced with 2 ml of complete growth medium. The following day, cells were passed into 0.8 mg/ml Geneticin (Gibco BRL). After several days, stable expressing clones were selected by observing cells for GFP expression under a fluorescence microscope and isolating colonies using 5-mm filter paper cloning discs soaked in trypsin/EDTA (Gibco BRL). High expressing colonies were expanded and frozen for further experiments.

Barbed End Assay

For the labeling of actin nucleation sites (barbed ends), a previously described protocol was used [Bailly et al., 1999; Chan et al., 1998]. In summary, cells were starved for 3 h and subsequently stimulated with EGF (final concentration 5 nM) for times as indicated on the x-axis of Figure 6, immediately followed by permeabilization with cytoskeletal buffer (0.45 μM of biotin-labeled G-actin [Cytoskeleton Inc.], 1% BSA, and 0.025 % saponin). The distribution of incorporated biotin-actin was identified using an anti-biotin, Cy5, coupled antibody (Jackson ImmunoResearch, West Grove, PA).

Live Cell Imaging

GFP-actin-expressing MTLn3 cells were plated on tissue culture dishes containing a coverslip (MatTek Corp.) for 24 h and serum starved for approximately 3 h before EGF stimulation. Cells were stimulated with a final concentration of 5 nM EGF at 37°C. GFP fluorescence images were taken for 5 min every 10 s starting 1 min before stimulation.

Phalloidin Staining

After fixation of the cells with 3.7% formaldehyde for 5 min at 37°C, cells were permeabilized with 0.5% Triton-X100 for 20 min, and washed with 0.1 M glycine for 10 min. Cells were blocked/stained in TBS with 1% BSA, 1% FCS, and 0.5 μM Alexa647-phalloidin for 30 min. Cells were rinsed five times for 5 min with TBS containing 1% BSA and mounted in 50% glycerol in TBS, supplemented with 6 mg/ml N-propyl gallate.

Light Microscopy and Fluorescence Quantification

All images for the barbed-end analysis and the live cell experiments were taken on an Olympus IX70 microscope using constant settings with 60× NA 1.4 infinity-corrected optics coupled to a computer-driven cooled

CCD camera (photometrics PXL KAF 1400 [Tucson, AZ] for in situ and SensiCam QE [Cooke Corp. MI] for in vivo experiments), using IP lab spectrum software (VayTek). All images were captured below saturation levels and analyzed by NIH image (program developed by the National Institute of Health, available on the internet at http://rsb.info.nih.gov/nih-image/) using a macro that traces cell perimeters by fluorescence threshold. The macro automated the collection of pixel intensity in a perimeter of the cell that started 1.54 μm outside the cell and extended 4.18 μm into the cell in 0.22-μum steps. For the measurement of barbed ends or the amount of F-actin in live cells in the leading edge of the lamellipodium (which has been described as the first 0.9 μm beyond the plasma membrane) [Chan et al., 2000], fluorescence intensity values for steps 0.22, 0.44, and 0.66 inside the cell were averaged. Also, the same data analysis conducted using fluorescence intensity values at the 0.22-step inside the cell yielded indistinguishable results. Previous experiments have shown that the extending leading edge of EGF stimulated MTLn3 cells is flat and of uniform thickness [Bailly et al., 1998a,b; Chan et al., 1998; Rotsch et al., 2001] and, thus, the contribution of the thickness of the cell to the fluorescence intensity is negligible, since the entire lamellipod is within the focal plane of the image taken.

Electron Microscopy

MTLn3 control cells and YFP-actin expressing stable clones of MTLn3 cells were grown on 5-mm coverslips, starved for 3 h, and then stimulated with EGF for 1 min. For preparation for electron microscopy, cells were permeabilized with 0.4% Triton X100 in cytoskeletal buffer for 1 min. After a rapid rinse with cytoskeletal buffer, further preparation was conducted as previously described, with minor modifications [Bailly et al., 1999]. Cells were fixed with 0.5% glutaraldehyde in cytoskeletal buffer for 10 min, rinsed in NH_4Cl in PBS buffer, incubated in 0.1% gelatin in PBS for 30 min, treated with 0.05% Triton in PBS for 1 min, rinsed four times in PBS, post-fixed with 1% glutaraldehyde for 15 min, and transferred to cytoskeletal buffer containing 5 μM phallacidin. To prepare samples for rotary shadow, the coverslips were transferred to distilled water with 5 μM phallacidin, washed twice with distilled water containing 0.1 μM phallacidin, and finally transferred to distilled water. As previously described [Bailly et al., 1999], coverslips were mounted on a rapid freezing apparatus (CF100; Life Cell Corp.) and frozen by slamming them into a liquid-nitrogen-cooled copper block. Samples were transferred to the specimen mount of a freeze fracture apparatus (CFE-50; Cressington) and rotary shadowed at a 45° angle with 1.2–1.3 nm tantalum-tungsten, and 2.5 carbon at 90°. The replicas were separated from the glass coverslips with 25% hydrofluoric acid, washed with distilled water, and picked up onto the surface of formvar-coated copper grids. Samples were examined using a JEOL 100CX transmission electron microscope at 100 kV.

Microinjection

Cells were grown on MatTek dishes as described above. Microinjection was performed on an Eppendorf semiautomatic microinjection system using Eppendorf Femtotips II as described before [Chan et al., 2000]. Antibodies (nonimmune rabbit IgG at 2 mg/ml or function blocking anti-cofilin antibody Ab286 at 3 mg/ml) were mixed with Texas Red dextran (Molecular Probes, Eugene, OR) to allow identification of microinjected cells.

Immunoblotting

Equal amounts of GFP-β-actin (GBA) actin and wt MTLn3 cells were lysed in TAP-lysis buffer (10 mM Hepes, 3 mM $MgCl_2$, 10 mM KCl, 5% glycerol, 0.5% NP40) containing protease inhibitors for 30 min on ice, separated by SDS-PAGE, and blotted to nitrocellulose membrane. Endogenous actin and GBA were detected by incubation with a polyclonal anti-actin (Cytoskeleton, CO) or a monoclonal anti-GFP antibody (Roche, Switzerland), respectively, followed by a peroxidase-conjugated secondary antibody. The bands were visualized and quantified by chemilluminescence of the peroxidase activity using the ECL-plus kit (Amersham, UK).

Actin Polymerization Assay

GBA MTLn3 cell were lysed in 200 μl of TAP-lysis buffer for 30 min on ice and centrifuged for 30 min using a Beckman airfuge at 20 psi to remove filamentous actin. After addition of 2 μM monomeric actin, the supernatant was transferred into a glass cuvette and the GFP fluorescence measured at 515 nm with a PTI QuantaMaster fluorescence spectrometer (PTI, NJ) at 30°C. GFP was excited at 490 nm. Nucleation was started after the addition of 2× actin nucleation buffer (buffer A: 2 mM Tris, 0.2 mM ATP, 0.5 mM DTT, 0.2 mM $CaCl_2$, 0.02% NaN_3 with addition of 4 mM $MgCl_2$, 100 mM KCl, and 0.4 mM EGTA). To confirm actin nucleation under these conditions, the solution was centrifuged a second time for 30 min to remove the newly polymerized F-actin and a reduction of the GBA fluorescence observed.

RESULTS

To develop a cell line that stably expresses GFP-β-actin at physiological levels, MTLn3 cells were transfected with a construct driving expression of the GFP-

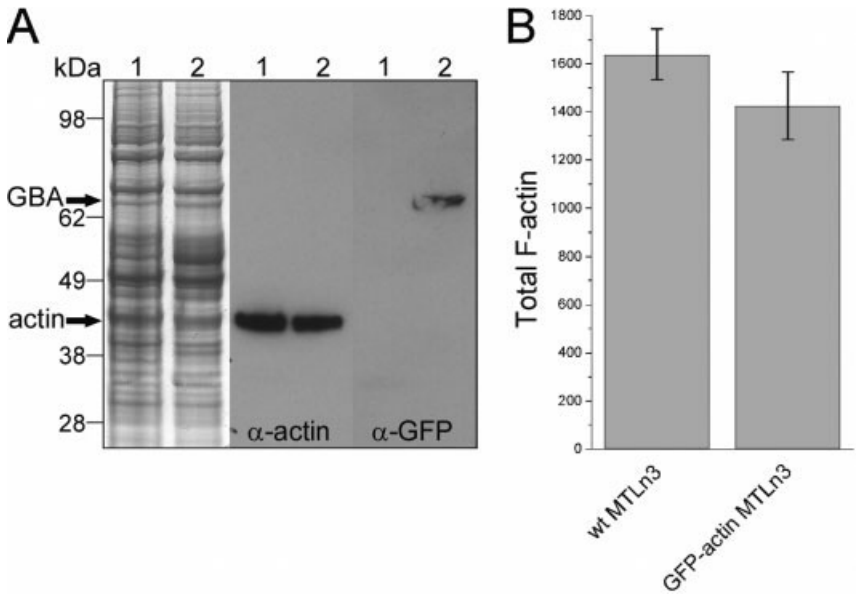

Fig. 1. The total actin level is not influenced by the expression of GFP-β-actin. **A:** Coomassie blue staining and Western blot of actin and GBA of wild-type and GBA expressing MTLn3 cells. Cell lysates of both cell types were separated by SDS-PAGE and immunoblotted with an anti-EGFP and polyclonal anti-actin antibody, respectively. The anti-actin antibody recognized just the endogenous actin in both cell lines with an apparent molecular weight of 43 kDa as described previously [Ballestrem et al., 1998]. No significant changes in the endogenous actin expression level were observed in GBA MTLn3 cells. Also the Coomassie blue staining of the whole cell lysate is similar and shows no obvious additional band at 70 kDa for GBA, indicating that the total actin level is unchanged. **B:** Wild-type MTLn3 and GBA expressing MTLn3 cells were stained with fluorescently labeled phalloidin for total F-actin concentration and the intensity detected by fluorescence microscopy. The total F-actin concentration in both cells is similar.

β-actin fusion protein (GBA) from the β-actin long promoter [Ballestrem et al., 1998].

The expression of GBA resulted in a minor suppression of the endogenous actin by approximately 5% as quantified from Western blot as well as Coomassie blue staining of the whole cell lysate of wt and GBA MTLn3 cells (Fig. 1A). Due to the fact that GBA is not recognized by anti-actin antibodies, as described previously [Ballestrem et al., 1998], the amount of GBA was estimated from the Coomassie staining only. The protein band at 70 kDa containing GBA, as indicated by immunoblotting against the green fluorescence protein (GFP), was slightly increased in the GBA expressing MTLn3 cells compared to the wt MTLn3 cells. Thus, the use of the wt β-actin long promoter resulted in nearly unchanged total actin expression at physiological level. In addition to the total actin concentration, we measured the amount of filamentous actin in wt and GBA MTLn3 cells (Fig. 1B). We stained both cell lines with Alexa633 conjugated phalloidin, measured the total cell fluorescence, and found no change in F-actin levels. Thus, both the total amount of actin as well as the amount of filamentous actin remained unchanged after transfection. This is important since the over-expression of GFP-actin can cause aggregation of actin and suppression of endogenous actin levels, both of which are toxic to the cells (data not shown).

MTLn3 cells were used in these experiments because EGF stimulation of these cells causes a well-characterized appearance of free barbed ends at the leading edge of lamellipods and the synchronous extension of the lamellipods over 3 min [Bailly et al., 1999; Chan et al., 2000]. The thinness of the lamellipods extended from the MTLn3 cells (~400–600 nm) [Rotsch et al., 2001] allows imaging of the entire depth of the lamellipod in a single focal plane. The free barbed ends that appear in response to EGF are only found in the nucleation zone, which is defined independently as a tropomyosin poor and cofilin and Arp2/3 complex rich zone directly adjacent to the leading edge [DesMarais et al., 2002].

Use of GBA expressing MTLn3 cells allowed comparison of barbed end measurements using two methods, time resolved fixation and live cell fluorescence time-lapse microscopy, in a well-characterized cell type. Figure 2 demonstrates the pattern of actin filaments in cells stably expressing physiological levels of GBA. Cells were fixed, extracted of G-actin, and stained with phalloidin over the 150 s time course of the EGF stimulated lamellipod extension response. The pattern of actin filaments observed by imaging the GBA signal is identical to that seen with phalloidin staining. The pattern of GBA in cells is identical before and after extraction of G-actin, indicating that G-actin does not contribute significantly to the GBA signal (see Fig. 2A and B). Furthermore, the

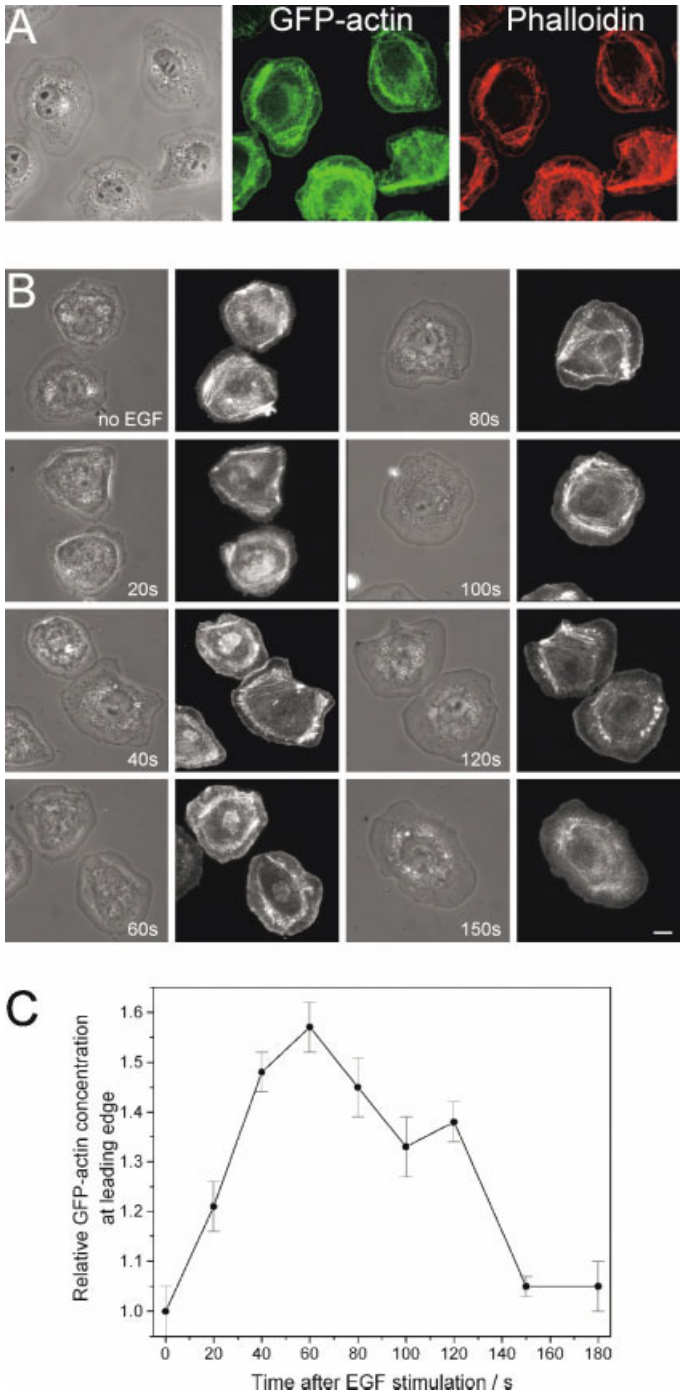

Fig. 2. GFP-β-actin faithfully defines actin filaments in cells before and after stimulation. GFP-β-actin (GBA) expressing MTLn3 cells were stimulated with EGF with a final concentration of 5 nM at 37°C and fixed at the time points shown. Monomeric actin was extracted during fixation. **A:** Distribution of GFP-actin and Alexa-648 phalloidin staining at 60 s after stimulation. The distribution of GFP-actin is identical with the phalloidin staining indicating the incorporation of GFP-actin in the stress fibers and the actin filaments in the nucleation zones at the leading edge. **B:** Phase and GFP fluorescent images of cells fixed at different time points after EGF stimulation show the distribution of F-actin during EGF-stimulated lamellipod extension. **C:** The fluorescence intensity of GBA at the leading edge was measured and normalized to the total fluorescence intensity of the whole cell to correct for different expression levels of GBA. A maximum of F-actin at the leading edge is reached at approximately 60 s after stimulation and is similar to that seen with phalloidin staining [Chan et al., 1998]. Error bars are s.e.m., n = 8–11 cells. Scale bar = 10 μm.

pattern of F-actin in cells imaged by GBA shows the well-characterized increase in F-actin in the nucleation zone at the leading edge during EGF-stimulated lamellipod extension, previously documented by time-resolved fixation methods [Chan et al., 1998; DesMarais et al., 2002], with a maximal accumulation of F-actin 60–80 s after EGF stimulation (Fig. 2B and C).

Figure 3 demonstrates the use of GBA to observe changes in F-actin in live cells before and after stimulation with EGF. The results are similar to those shown in Figure 2 and illustrate the usefulness of using GBA to define changes in F-actin at the leading edge during lamellipod extension in live cells. Increases in F-actin at the leading edge were measured in fixed and living cells (compare Figs. 2C and 3B). Both techniques have similar signal to background, but a higher temporal resolution is achieved with the live cell fluorescence time-lapse method. In each case, maximal

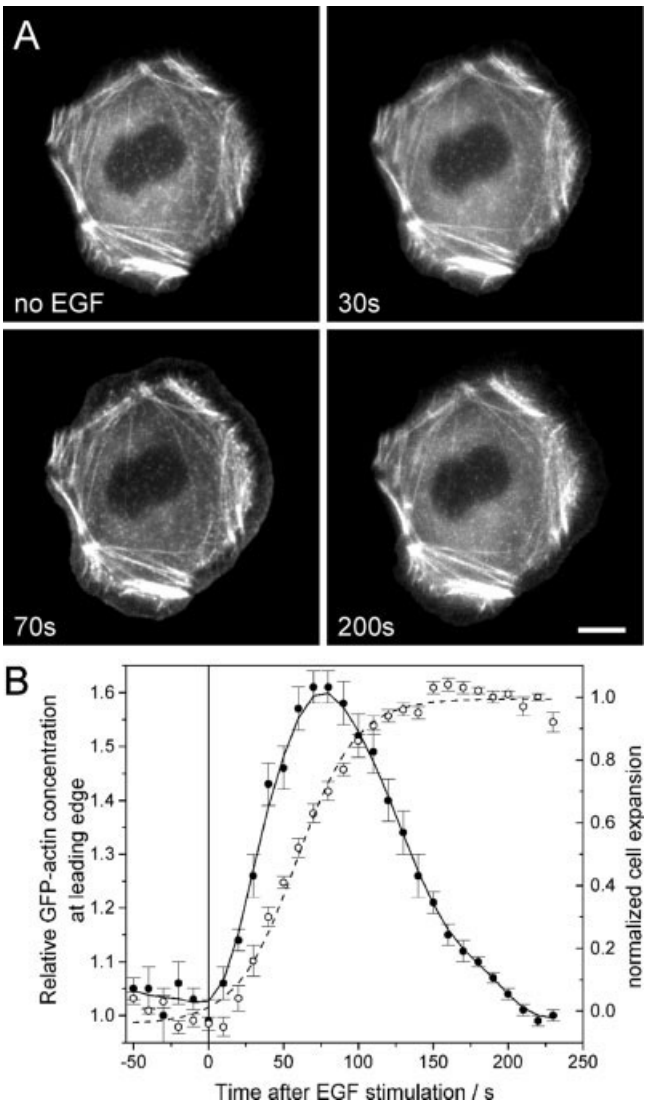

Fig. 3. The live cell fluorescence time lapse method can be used with GBA to measure changes in F-actin during cell motility. **A:** Images of GBA expressing MTLn3 cells were taken every 10 s for 1 min before and up to 4 min after EGF stimulation at 37°C. The pattern of changes in F-actin during lamellipod extension is similar to that seen with the time-resolved fixation method (Fig. 2). **B:** The F-actin concentration at the cell edge is maximal at 70–80 s after stimulation with EGF (*solid line*) while the lamellipod extension plateaus approximately 40 s later at 2 min after stimulation (*dashed line*). After 3 min, the F-actin concentration at the cell edge reaches the pre-stimulation level. Error bars are s.e.m., n = 9 cells. Scale bar = 10 μm.

accumulation of F-actin occurred 60–80 s after stimulation.

In order to show that the observed increased GFP fluorescence is caused by a nucleation event at the leading edge and not by alteration of the GFP fluorescence signal by, e.g., protein binding, we analyzed the content of fluorescent actin in the leading edge compartment and in stress fibers of GBA MTLn3 cells and compared this

TABLE I. Fraction of GFP-β-Actin and F-Actin (Rhodamine Phalloidin Staining) in the Leading Edge and in Stress Fibers of MTLn3 Cells

	GFP-β-actin (GBA, %)	F-actin (rhodamine phalloidin, %)
Leading edge	7 ± 2	9[a]
Stress fibers	49 ± 19	59[a]

[a]From DesMarais et al. [2002].

to previous measurements by fluorescent phalloidin staining in wt MTLn3 cells (Table I) [DesMarais et al., 2002]. In both cases, a similar distribution of either GBA- or phalloidin-stained actin is present in the leading edge compartment (around 9%) and in stress fibers (49–59%) 3 min after EGF stimulation. Since both compartments have different protein compositions, this indicates that (1) the GFP fluorescence is not significantly altered by protein binding to F-actin and again (2) that the addition of GFP to actin does not change the cellular distribution of actin.

To determine if the GFP fluorescence intensity of GBA changes during nucleation, we measured the GFP fluorescence intensity of monomeric GBA before and during nucleation in vitro (Fig. 4). GBA MTLn3 cell lysate was centrifuged to remove filamentous actin. To the supernatant containing monomeric GBA, we added 2 μM G-actin to increase the actin concentration above the critical concentration that is necessary for nucleation. Nucleation was started by addition of high-salt buffer and the GFP fluorescence intensity detected over time. The GFP fluorescence increased slightly by 2.7 ± 1.1% during nucleation, which is small compared to the observed fluorescence signal change at the leading edge after stimulation (see Fig. 3B). After a second centrifugation step, the fluorescence signal in the supernatant decreased, indicative of actin nucleation in this assay. It has been shown previously that EGFP fluorescence is stable between pH 7.0 and 11 [Patterson et al., 1997] and, thus, the GFP fluorescence is nearly inert against pH changes, protein binding, or actin nucleation and can be used to quantify filamentous actin in different compartments of the cell.

The morphology of actin filaments in the dynamic leading edge actin compartment was determined in cells expressing just wt actin or GBA using electron microscopy. As shown in Figure 5, cells stimulated with EGF for 1 min, fixed, and rotary shadowed to contrast actin filaments contained the same filament density, filament thickness, and overall filament appearance, indicating that GBA does not alter the morphology of the dendritic actin network at the leading edge (wt cells: Fig. 5A and B; GBA expressing cells: Fig. 5C and D).

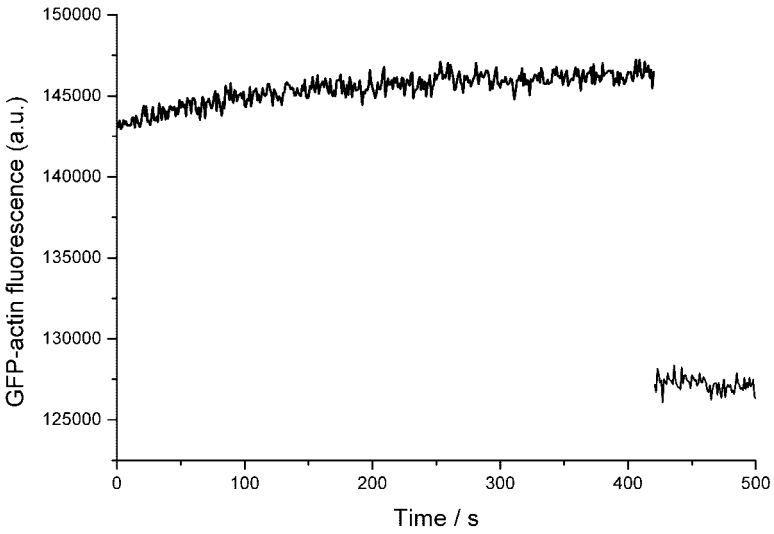

Fig. 4. GBA retains its fluorescence in filamentous actin GBA MTLn3 cells where extracted and the F-actin was pelleted by microcentrifugation. The supernatant retaining the monomeric GBA and unlabeled actin was complemented with 2 μM purified G-actin to increase the actin concentration above the critical concentration and the GFP fluorescence was measured during polymerization in a fluorescence spectrometer at 30°C. The fluorescence intensity increased slightly by 2.7 ± 1.1% in filamentous actin. To show actin polymerization under these conditions, we pelleted the newly polymerized filamentous actin and observed a decreased fluorescence intensity in the supernatant.

In order to measure free barbed end numbers in live cells using GBA and live cell fluorescence time-lapse microscopy, we took advantage of several properties of resting cells. First, in cells that are not rapidly moving, such as MTLn3 cells, the resting G-actin concentration is not limiting and is approximately 77 μM [Chan et al., 1998; Edmonds et al., 1996]. After stimulation of cell motility with EGF, the G-actin concentration falls to 54 μM [Chan et al., 1998; Edmonds et al., 1996]. Since the G-actin concentration is buffered in the cytoplasm by binding to profilin and thymosin beta 4 [Pollard et al., 2000] and profilin binding at low concentrations favors elongation at barbed ends [Bubb et al., 2003] but prevents elongation at the pointed end of F-actin [Pring et al., 1992], elongation of barbed ends will dominate in vivo until the G-actin concentration falls and filament disassembly begins. Free profilin is believed to remain at low concentration in resting cells due to PIP_2 binding [Goldschmidt-Clermont et al., 1990]. Under these conditions, filamentous actin (N_f) depends on the number of barbed ends ($N_{barbed\ ends}$), the concentration of monomeric actin (c_m), and the depolymerization rate at the pointed ends (Eq. 1). K^+_{on} and k^-_{off} are the polymerization and depolymerization rate constants at the barbed and pointed ends, respectively.

$$N_f = (N_{barbed\ ends} k^+_{on} c_m - N_{pointed\ ends} k^-_{off}) \cdot t \quad (1)$$

In resting cells the amount of filamentous actin is constant; this means the polymerization and depolymerization rates are the same (Eq. 2). While the polymerization rate increases after EGF stimulation, the depolymerization rate remains unchanged. Thus, the change of the amount of filamentous actin is equal to the increase of barbed ends $\Delta N_{barbed\ ends}$ and G-actin concentration (Eq. 3). $\Delta N_{barbed\ ends}$ is the difference of barbed ends in resting cells before and after EGF stimulation.

$$\frac{dN_f}{dt} = 0 \Rightarrow N^0_{barbed\ end} k^+_{on} c_m = N^0_{pointed\ end} k^-_{off} \quad (2)$$

$$\frac{dN_f}{dt} = \Delta N_{barbed\ ends} k^+_{on} c_m \quad (3)$$

The time it takes to deplete G-actin in vivo has been estimated to be on the minute time scale using jasplakinolide inhibition of motility [Cramer, 1999]. Since the facilitated diffusion rate of G-actin in lamellipods is not limiting for polymerization and can be 5 times that of the rate of diffusion of G-actin in vitro [Zicha et al., 2003], the initial rate of polymerization in resting cells will not be limited by G-actin concentrations and will only occur on free barbed ends (Eq. 4).

$$\frac{dN_f}{dt} \propto \Delta N_{barbed\ ends} \quad (4)$$

While the GFP-fluorescence in actin filaments is proportional to the amount of filamentous actin (Eq. 5), the first derivative of the GFP-fluorescence gives the relative increase of barbed ends (Eq. 6).

$$F_{GFP} \propto N_f \quad (5)$$

$$\frac{dF_{GFP}}{dt} \propto \Delta N_{barbed\ ends} \quad (6)$$

Therefore, by measuring the increase of GBA fluorescence at the leading edge over time, it should be possible to determine the relative increase of barbed ends in vivo.

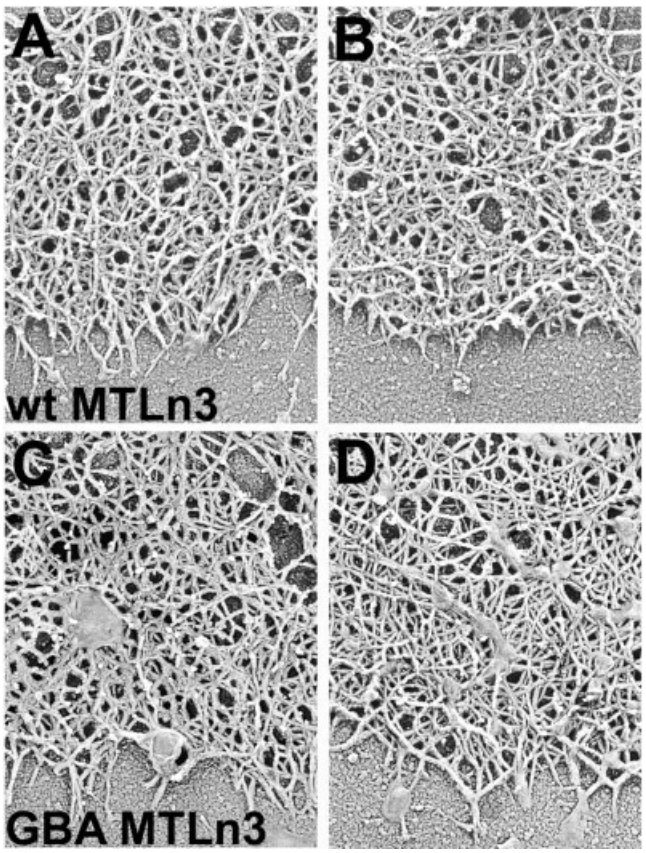

Fig. 5. Actin filaments in lamellipods are not altered in cells expressing GBA. Wild type and GBA-expressing MTLn3 cells were stimulated with EGF for 1 min, fixed, extracted, and rotary shadowed for electron microscopy. Two typical examples each of the actin filament networks in leading edges of wild-type (**A,B**) and GBA-expressing cells (**C,D**) are shown.

To evaluate the use of GBA to measure barbed ends in vivo, the number of free barbed ends measured after the stimulation of actin polymerization in resting MTLn3 cells was compared using the time-resolved fixation and live cell fluorescence time-lapse microscopy methods. The direct measurement of barbed ends in MTLn3 cells using the time-resolved fixation method with biotin-labeled G-actin is shown in Figure 6A and C. In these experiments, biotin-labeled actin was incorporated in newly polymerized actin filaments and stained with Alexa647-labeled biotin-antibody. Scoring of the fluorescence in the nucleation zone shows that barbed ends appeared in several unresolved peaks, with the initial transient being the major peak at 40–60 s. This early actin polymerization transient has been documented previously and corresponds to the beginning of leading edge assembly and lamellipod extension [Bailly et al., 1999; Chan et al., 2000]. The later polymerization transients are not well understood and may be involved in protrusive force, filament turnover, and focal adhesion formation.

Barbed ends were also measured in the nucleation zone using the live cell fluorescence time-lapse microscopy method. As shown in Figure 6B and C, the barbed ends measured by calculating the first derivative of the change in F-actin fluorescence at the leading edge vs. time predicts an early increase in free barbed ends identical in appearance and duration to that observed with the time-resolved fixation method. However, after the initial increase in actin polymerization ends at approximately 60 s, the live cell fluorescence time-lapse microscopy method fails to follow the later changes in free barbed end number observed with the time-resolved fixation method. Since the cessation of actin polymerization is complex in living cells and does not involve a single kinetic process, it is not possible to measure barbed end number from changes in fluorescence in live cells past the initial increase in polymerization.

One of the factors involved in actin polymerization at the leading edge is cofilin, which can depolymerize and sever actin filaments and is enriched in the nucleation zone at the plasma membrane of MTLn3 cells [Chan et al., 2000; Ichetovkin et al., 2000]. The severing activity of cofilin is thought to increase the number of barbed ends upon EGF stimulation and, thus, increase actin polymerization in the nucleation zone. It has previously been shown that microinjection of a function blocking anti-cofilin antibody (Ab286) inhibits the protrusion of the lamellipod upon EGF treatment and also inhibits barbed ends formation as measured using the biotin-actin incorporation method in fixed cells [Chan et al., 2000]. To test our method of following the incorporation of GBA in the nucleation zone as an indicator of barbed ends in live cells, we microinjected this anti-cofilin antibody into live MTLn3 cells (Fig. 7). Figure 7A shows a representative control injected live cell before EGF stimulation and 70 s after EGF stimulation, at which time there is maximal incorporation of GBA at the leading edge. In contrast, the anti-cofilin microinjected live cell in Figure 7B does not exhibit an increase of GBA at the leading edge after EGF stimulation, indicating a lack of barbed end formation due to inhibition of cofilin. The quantitation shown in Figure 7C indicates a fourfold decrease of GBA incorporation in anti-cofilin-injected cells compared to control cells corresponding to a decreased amount of barbed end formation in cofilin-inhibited cells.

DISCUSSION

We have developed a new live cell fluorescence time-lapse microscopy method to measure the relative number of free barbed ends that are generated to initiate

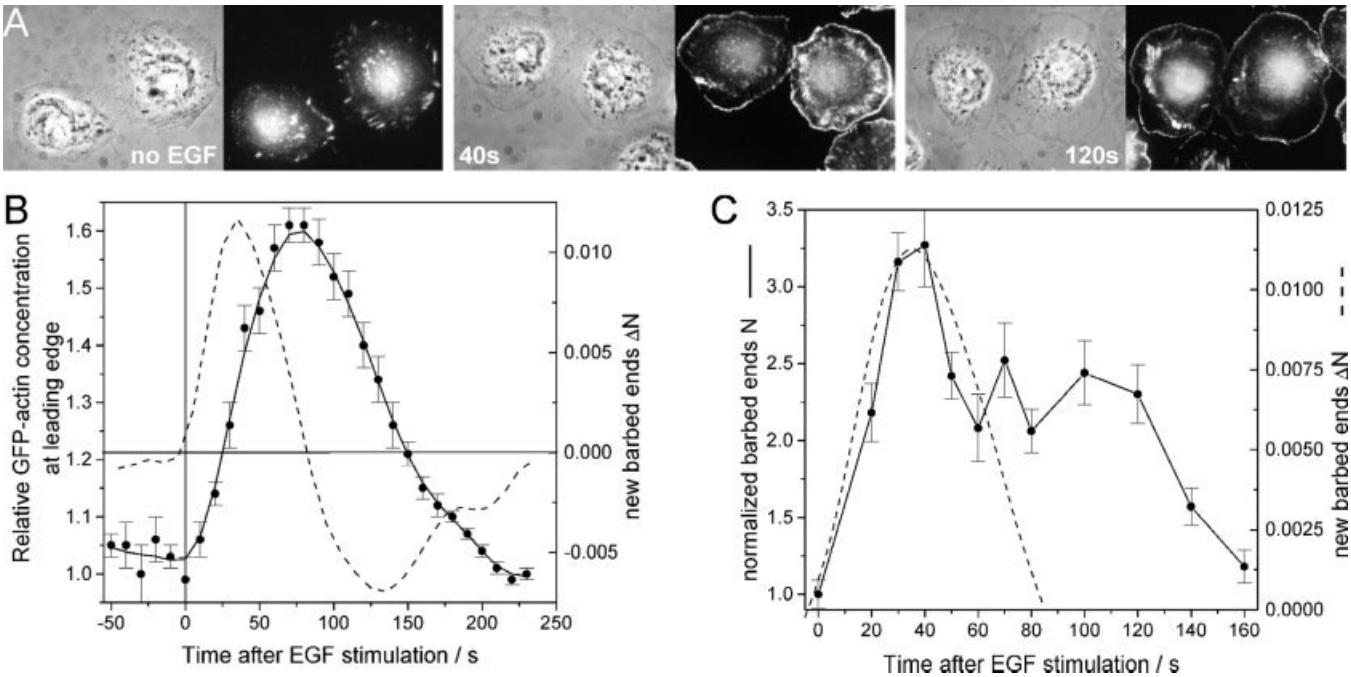

Fig. 6. Time-resolved fixation and live cell fluorescence time-lapse microscopy give similar measures of the initial free barbed ends during lamellipod extension. Time-resolved fixation (**A,C**): Free barbed ends were detected as new G-actin incorporation into saponin permeabilized cells at various times as indicated after EGF stimulation [Chan et al., 1998]. **A:** Images of phase microscopy and biotin-labeled actin incorporation after EGF stimulation were obtained by stimulating at 37°C with EGF, immediately permeabilizing and adding biotin-labeled G-actin for 1 min. **C:** The fluorescence intensity at the leading edge was measured from the membrane to 0.2 μm into the cell and plotted as a function of time after stimulation (*solid line*). The fluorescence intensity is proportional to the number of barbed ends present in the measured compartment [Bailly et al., 1999; Chan et al., 2000]. The number of free barbed ends reaches a maximum at approximately 30–40 s after stimulation. Error bars are s.e.m., n=25-30 cells. Live cell fluorescence time-lapse microscopy (**B,C**): Determination of the number of free barbed ends in live cells using GBA. **B:** The change in F-actin amount in the nucleation zone was measured as the increase in GBA fluorescence intensity and plotted vs. time after EGF stimulation (*solid line*). The initial number of barbed ends is proportional to the actin polymerization rate and is the 1st derivative of the GBA fluorescence plot (*solid line*) and is shown as the *dashed line*. The F-actin amount at the leading edge reaches a maximum at 70–80 s (*solid line*) while the number of barded ends is maximal at 30–40 s after stimulation (*dashed line*). **C**: Comparison of the free barbed ends measured with the live cell fluorescence time-lapse microscopy method (*dashed line*) with time-resolved fixation method (*solid line*). Both methods measure the same kinetic of barbed end appearance during the initial stage of polymerization.

lamellipod protrusion in cells after EGF stimulation. In this work, we used cell lines (MTLn3) that stably express GBA, avoiding vast over-expression of GBA, which may alter cell morphology. This cell line can be triggered to resume motility in an experimentally defined way. GBA-expressing cells were stimulated to initiate protrusion or motility, which was followed by time-lapse microscopy. The edge intensity of GBA was measured for each time-point and graphed as a function of time. Under the experimental conditions described, the GFP-edge-fluorescence measured is proportional to the amount of filamentous actin, and the rate of F-actin incorporation, which is the first derivative of the change in GFP-fluorescence over time, gives the relative amount of barbed ends.

This method avoids permeabilization of cells and, therefore, a possible extraction and/or re-localization of dynamic filaments and their associated proteins. This has always been an issue in the time-resolved fixation method, which has been used extensively to follow barbed end dynamics in cells [Bailly et al., 1999; Chan et al., 1998, 2000; Symons and Mitchison 1991], but has been criticized for introducing potential artifacts due to the harsh permeabilization step. The live cell fluorescence time-lapse microscopy method circumvents this problem when measuring initial polymerization transients in dynamic and labile filament populations. Altogether, advantages of this new approach include: (1) it is a non-destructive method with (2) a higher temporal resolution than fixation methods. An attractive feature of this method is (3) that the measurement is made in live cells allowing the history and progress of the cell to be followed before and after stimulation of motility, while measuring the relative amount of barbed ends. (4) Quantification is more straightforward since few numbers of cells are necessary to observe a given phenotype. For

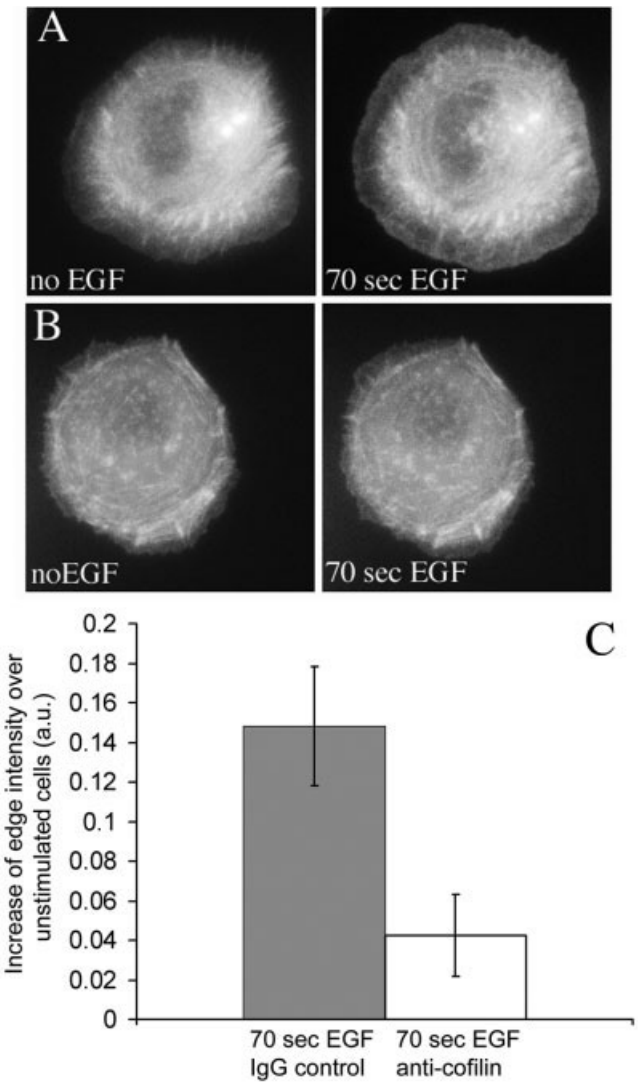

Fig. 7. Inhibition of cofilin prevents GBA accumulation in live MTLn3 cells after EGF stimulation. **A:** Images of a control IgG injected MTLn3 cell expressing GBA before and after 70 s of EGF stimulation. **B:** Images of a GBA expressing, anti-cofilin function blocking antibody (Ab286) injected MTLn3 cell before and after 70 s of EGF stimulation. **C:** The F-actin amount in the nucleation zone was measured as the GBA fluorescence intensity in this zone in unstimulated live cells and after EGF stimulation. The graph shows the increase of fluorescence intensity at 70 s of EGF stimulation over unstimulated cells. Error bars are s.e.m., n=15 for IgG control cells and n = 17 for anti-cofilin injected cells.

example, when microinjection of limiting reagents, such as antibodies, is necessary, use of the reagent is maximized in this live cell method, since each microinjected cell yields data over an entire time-course; thus, a total of 10–15 cells may yield the required data. In fixed cell methods, each time-point may require a minimum of 10–15 cells; thus, in order to generate an entire time-course, hundreds of microinjected cells would be necessary. However, one has to keep in mind that the method is only applicable to follow initial actin polymerization transients, since later actin polymerization transients cannot be deconvolved into barbed end measurements with confidence, since the relative contributions of polymerization and depolymerization to the transient are not well defined beyond the initial transient.

As an example of application, we have microinjected cells with a function blocking anti-cofilin antibody. Cofilin is one of the factors that have been implicated to play a role in the regulation of cell motility. It has previously been shown that upon EGF stimulation, the anti-cofilin function-blocking antibody inhibits lamellipod protrusion and the generation of barbed ends as measured with the fixed cell barbed end assay that utilizes cell permeabilization [Chan et al., 2000]. Here we show that microinjection of this antibody into living cells decreases the GBA edge intensity 70 s after EGF stimulation, which indicates that there has been a decrease in barbed end formation due to inhibition of cofilin function.

This live-cell barbed end method is particularly suitable for use in experiments where triggered polymerization in live cells must be followed with high temporal resolution such as in uncaging, FRET and FRAP analyses, and studies of chemotaxis. It is also an advantage when measuring the initiation of motility by hormone stimulation and in cells microinjected with antibodies and plasmids designed to either inhibit or stimulate motility. This method should find broad appreciation in cells where very rapid changes in the dynamic filament population are to be measured, particularly in cells where permeabilization may cause extraction and/or change in location of the dynamic filaments.

ACKNOWLEDGMENTS

We thank B. Imhof (Department of Pathology, Centre Medical Universitaire, Geneva, Switzerland) for his generous gift of the GFP-β-actin plasmid. This work was supported by grants from the NIH to J.C. and R.H.S.

REFERENCES

Bailly M, Condeelis JS, Segall JE. 1998a. Chemoattractant-induced lamellipod extension. Microsc Res Tech 43:433–443.

Bailly M, Yan L, Whitesides GM, Condeelis JS, Segall JE. 1998b. Regulation of protrusion shape and adhesion to the substratum during chemotactic responses of mammalian carcinoma cells. Exp Cell Res 241:285–299.

Bailly M, Macaluso F, Cammer M, Chan A, Segall JE, Condeelis JS. 1999. Relationship between Arp2/3 complex and the barbed ends of actin filaments at the leading edge of carcinoma cells after epidermal growth factor stimulation. J Cell Biol 145:331–345.

Ballestrem C, Wehrle-Haller B, Imhof BA. 1998. Actin dynamics in living mammalian cells. J Cell Sci 111:1649–1658.

Bubb MR, Yarmola EG, Gibson BG, Southwick FS. 2003. Depolymerization of actin filaments by profilin. Effects of profilin on capping protein function. J Biol Chem 278:24629–24635.

Chan AY, Raft S, Bailly M, Wyckoff JB, Segall JE, Condeelis JS. 1998. EGF stimulates an increase in actin nucleation and filament number at the leading edge of the lamellipod in mammary adenocarcinoma cells. J Cell Sci 111:199–211.

Chan AY, Bailly M, Zebda N, Segall JE, Condeelis JS. 2000. Role of cofilin in epidermal growth factor-stimulated actin polymerization and lamellipod protrusion. J Cell Biol 148:531–542.

Condeelis J. 2001. How is actin polymerization nucleated in vivo? Trends Cell Biol 11:288–293.

Cramer LP. 1999. Role of actin-filament disassembly in lamellipodium protrusion in motile cells revealed using the drug jasplakinolide. Curr Biol 9:1095–1105.

DesMarais V, Ichetovkin I, Condeelis J, Hitchcock-DeGregori SE. 2002. Spatial regulation of actin dynamics: a tropomyosin-free, actin-rich compartment at the leading edge. J Cell Sci 115: 4649–4660.

Edmonds BT, Wyckoff J, Yeung YG, Wang Y, Stanley ER, Jones J, Segall J, Condeelis J. 1996. Elongation factor-1 alpha is an overexpressed actin binding protein in metastatic rat mammary adenocarcinoma. J Cell Sci 109:2705–2714.

Goldschmidt-Clermont PJ, Machesky LM, Baldassare JJ, Pollard TD. 1990. The actin-binding protein profilin binds to PIP2 and inhibits its hydrolysis by phospholipase C. Science 247:1575–1578.

Hartwig JH, Bokoch GM, Carpenter CL, Janmey PA, Taylor LA, Toker A, Stossel TP. 1995. Thrombin receptor ligation and activated Rac uncap actin filament barbed ends through phosphoinositide synthesis in permeabilized human platelets. Cell 82:643–653.

Ichetovkin I, Han J, Pang KM, Knecht DA, Condeelis JS. 2000. Actin filaments are severed by both native and recombinant dictyostelium cofilin but to different extents. Cell Motil Cytoskeleton 45:293–306.

Patterson GH, Knobel SM, Sharif WD, Kain SR, Piston DW. 1997. Use of the green fluorescent protein and its mutants in quantitative fluorescence microscopy. Biophys J 73:2782–2790.

Pollard TD, Blanchoin L, Mullins RD. 2000. Molecular mechanisms controlling actin filament dynamics in nonmuscle cells. Annu Rev Biophys Biomol Struct 29:545–576.

Pring M, Weber A, Bubb MR. 1992. Profilin-actin complexes directly elongate actin filaments at the barbed end. Biochemistry 31: 1827–1836.

Pruyne D, Evangelista M, Yang C, Bi E, Zigmond S, Bretscher A, Boone C. 2002. Role of formins in actin assembly: nucleation and barbed-end association. Science 297:612–615.

Rotsch C, Jacobson K, Condeelis J, Radmacher M. 2001. EGF-stimulated lamellipod extension in adenocarcinoma cells. Ultramicroscopy 86:97–106.

Segall JE, Tyerech S, Boselli L, Masseling S, Helft J, Chan A, Jones J, Condeelis J. 1996. EGF stimulates lamellipod extension in metastatic mammary adenocarcinoma cells by an actin-dependent mechanism. Clin Exp Metast 14:61–72.

Symons MH, Mitchison TJ. 1991. Control of actin polymerization in live and permeabilized fibroblasts. J Cell Biol 114:503–513.

Theriot JA, Mitchison TJ. 1992. Comparison of actin and cell surface dynamics in motile fibroblasts. J Cell Biol 119:367–377.

Watanabe N, Mitchison TJ. 2002. Single-molecule speckle analysis of actin filament turnover in lamellipodia. Science 295:1083–1086.

Waterman-Storer CM, Salmon ED. 1997. Actomyosin-based retrograde flow of microtubules in the lamella of migrating epithelial cells influences microtubule dynamic instability and turnover and is associated with microtubule breakage and treadmilling. J Cell Biol 139:417–434.

Zicha D, Dobbie IM, Holt MR, Monypenny J, Soong DY, Gray C, Dunn GA. 2003. Rapid actin transport during cell protrusion. Science 300:142–145.